J Mater Sci: Mater Med (2011) 22:2791–2802
DOI 10.1007/s10856-011-4444-y

Preparation of chitosan films using different neutralizing solutions to improve endothelial cell compatibility

Qing He · Qiang Ao · Yandao Gong · Xiufang Zhang

Received: 11 May 2011 / Accepted: 5 September 2011 / Published online: 1 November 2011

Abstract The development of chitosan-based constructs for application in large-size defects or highly vascularized tissues is still a challenging issue. The poor endothelial cell compatibility of chitosan hinders the colonization of vascular endothelial cells in the chitosan-based constructs, and retards the establishment of a functional microvascular network following implantation. The aim of the present study is to prepare chitosan films with different neutralization methods to improve their endothelial cell compatibility. Chitosan salt films were neutralized with either sodium hydroxide (NaOH) aqueous solution, NaOH ethanol solution, or ethanol solution without NaOH. The physicochemical properties and endothelial cell compatibility of the chitosan films were investigated. Results indicated that neutralization with different solutions affected the surface chemistry, swelling ratio, crystalline conformation, nanotopography, and mechanical properties of the chitosan films. The NaOH ethanol solution-neutralized chitosan film (Chi-NaOH/EtOH film) displayed a nanofiber-dominant surface, while the NaOH aqueous solution-neutralized film (Chi-NaOH/H_2O film) and the ethanol solution-neutralized film (Chi-EtOH film) displayed nanoparticle-dominant surfaces. Moreover, the Chi-NaOH/EtOH films exhibited a higher stiffness as compared to the Chi-NaOH/H_2O and Chi-EtOH films. Endothelial cell compatibility of the chitosan films was evaluated with a human microvascular endothelial cell line, HMEC-1. Compared with the Chi-NaOH/H_2O and Chi-EtOH films, HMECs cultured on the Chi-NaOH/EtOH films fully spread and exhibited significantly higher levels of adhesion and proliferation, with retention of the endothelial phenotype and function. Our findings suggest that the surface nanotopography and mechanical properties contribute to determining the endothelial cell compatibility of chitosan films. The nature of the neutralizing solutions can affect the physicochemical properties and endothelial cell compatibility of chitosan films. Therefore, selection of suitable neutralization methods is highly important for the application of chitosan in tissue engineering.

Q. He · Y. Gong · X. Zhang (✉)
State Key Laboratory of Biomembrane and Membrane Biotechnology, School of Life Sciences, Tsinghua University, Beijing 100084, China
e-mail: zxf-dbs@mail.tsinghua.edu.cn

Q. Ao
Institute of Neurological Disorders, Tsinghua University, Beijing 100049, China

1 Introduction

Chitosan, α (1 → 4)-2-amino-2-deoxy-β-D-glucan, is a cationic natural polysaccharide obtained by the *N*-deacetylation of chitin under alkaline conditions. Chitosan has been considered a promising biomaterial in tissue engineering for cartilage [1], bone [2], peripheral nerves [3], etc., due to its good biocompatibility and biodegradability. However, the development of chitosan-based constructs for application in large-size defects or highly vascularized tissues is still a challenging issue. A major limitation is associated with the inability to supply sufficient oxygen and nutrients to the inner part of the cell–chitosan constructs in the early stage after implantation [4]. If located more than a few hundred microns away from the nearest capillaries, the cells in the constructs become hypoxic and enter apoptosis, resulting in poor cell survival.

To resolve this problem, a number of strategies are being developed. One of the promising approaches is to pre-colonize the matrices with vascular endothelial cells [5]. The pre-vascularization is expected to contribute to the establishment of a functional capillary network able to deliver oxygen and nutrients throughout the constructs following implantation. Successful formation of a functional microvasculature relies on the ability of the matrices to allow adhesion and proliferation of the vascular endothelial cells, as well as to support the endothelial phenotype and function. Unfortunately, the feasibility of chitosan material to be colonized by endothelial cells in vitro is not evident. It is reported that endothelial cells seeded on chitosan two-dimensional (2-D) films [6, 7] and three-dimensional (3-D) scaffolds [8] exhibited poor cell adhesion, spreading, and proliferation. Therefore, the endothelial cell compatibility of chitosan needs to be improved. The effects of chitosan physicochemical characteristics on the endothelial cell behavior should be further investigated.

Chitosan is a semicrystalline polysaccharide and is normally insoluble in aqueous solutions with pH value above 7. However, the free amino groups are protonated and the molecules become soluble in dilute acids (pH < 6). This pH-dependent solubility of chitosan provides a convenient method for its processing under mild conditions. Generally, chitosan is dissolved in acidic solution to form chitosan solution. With this solution chitosan films and porous scaffolds are fabricated by air drying and freeze drying, respectively. Then, the samples are commonly neutralized in either sodium hydroxide (NaOH) aqueous solution [6, 7, 9] or ethanol solution [8, 10]. The neutralization is a necessary step before the rehydration of the chitosan matrices. However, there is still very limited information about the effects of the different neutralization methods on physicochemical properties and cytocompatibility of chitosan.

This study is aimed to prepare chitosan films with good endothelial cell compatibility. The chitosan films were neutralized with either NaOH aqueous solution, NaOH ethanol solution, or ethanol solution without NaOH. For the first time, the effects of different solutions used for neutralization on the physicochemical properties and endothelial cell compatibility of chitosan films were investigated. The possible mechanisms were discussed.

2 Materials and methods

2.1 Materials

Chitosan (MW 500 kDa, deacetylation degree 85%) was supplied by Qingdao Haisheng Co., Ltd. (Qingdao, China). Mouse anti-human CD31 (MAB2148) and mouse anti-human E-selectin (MAB2150) were obtained from Millipore. Rabbit anti-human von Willebrand Factor (vWF) (A0082) was obtained from Dako. Tumor necrosis factor-α (TNF-α) and recombinant human vascular endothelial growth factor ($VEGF_{165}$) were obtained from PeproTech. Acetylated low density lipoprotein labeled with 1, 1′-dioctadecyl-3, 3, 3′, 3′-tetramethylindo-carbocyanine perchlorate (DiI-Ac-LDL) was purchased from Biomedical Technologies Inc. (Stoughton, USA). Matrigel was obtained from BD Biosciences (Bedford, USA). All other reagents were of analytical grade.

2.2 Preparation of chitosan films

Chitosan was dissolved at 2% (w/v) in 1.2% (v/v) acetic acid solution. The resulting chitosan solution was cast on glass cover slips or culture dishes, and then was dried at 50°C for 24 h to form thin films. After drying, the films were neutralized with either NaOH aqueous solution, NaOH ethanol solution, or ethanol solution without NaOH. For the first method, NaOH was dissolved at 2% (w/v) in deionized water. Chitosan films were immersed in this solution for 30 min and then washed with deionized water for three times. The films neutralized with this method were abbreviated as Chi-NaOH/H_2O. For the second method, ethanol was mixed with deionized water to make an 80% (v/v) ethanol solution, and then NaOH was dissolved at 2% (w/v) in the ethanol solution. Chitosan films were immersed in this solution for 30 min and then washed with 80% (v/v) ethanol solution for three times. The films neutralized with this method were abbreviated as Chi-NaOH/EtOH. For the third method, chitosan films were washed with 80% (v/v) ethanol solution without NaOH for four times (10 min each). The films neutralized with this method were abbreviated as Chi-EtOH. All the films were washed with phosphate buffer solution (PBS, pH 7.2) before cell seeding.

2.3 Attenuated total reflection fourier transform infrared (ATR-FTIR) spectrometry

FTIR spectra of chitosan films neutralized in different solutions were collected with a fourier transform infrared spectrometer (Spectrum GX, Perkin Elmer, USA) in the reflection mode. An attenuated total reflection accessory was used for all IR spectral acquisitions.

2.4 Swelling ratio measurement

Chitosan films were immersed in deionized water at room temperature until equilibrium was achieved. The films were then blotted with filter paper and weighed. Subsequently,

the films were dried at 60°C to a constant weight. The swelling ratio was determined by Eq. 1:

$$\text{Swelling ratio} = \frac{W_s - W_d}{W_d} \times 100\% \quad (1)$$

where W_s is the weight of the swollen film at equilibrium and W_d is the weight of the dried film.

2.5 X-ray diffraction (XRD) spectrometry

XRD patterns of chitosan films were measured using an X-ray diffractometer (Model D8 Advance, Bruker, Germany) with Ni-filtered Cu radiation operated at 30 kV and 30 mA as the X-ray source. The diffraction patterns were recorded over a range of diffraction angle $2\theta = 6$ to 40° at a scanning rate of 1° (2θ) per min and a step size of 0.1° (2θ).

2.6 Surface topography characterization by atomic force microscopy (AFM)

Topographies of chitosan films were observed with an atomic force microscope (PicoScan, Molecular Imaging, USA). Measurements were performed in contact mode under ambient conditions with silicon tips (CSC11, Silicon-MDT, Russia) at a scanning rate of 3 lines/s. For each sample, three random regions were examined with a scan size of 4 × 4 μm^2. And at least three samples were measured for each kind of chitosan film. The obtained AFM images were analyzed by the free software WSxM 4.0 (Develop 8.6).

2.7 Mechanical properties measurement

The mechanical properties of chitosan films were evaluated by a tensile test using a Universal Testing Machine (model AG-1, Shimadazu, Japan) equipped with a load cell of 50 N. The films were cut to 5 × 1 cm and immersed in deionized water until equilibrium before testing. All tests were performed at room temperature and the tensile speed was 0.5 cm/min. The elastic modulus, elongation-at-break, and tensile maximum strength were calculated from the stress–strain curves. The reported data was the average of five samples.

2.8 Endothelial cell compatibility of chitosan films

2.8.1 Cell culture

Human microvascular endothelial cell line (HMEC-1) used for this study was donated from Shanghai Institute of Materia Medica (Shanghai, China). The cell line was established by Ades et al. [11] through transfection of human dermal microvascular endothelial cells with a simian virus (SV) 40 T antigen for immortalization. The cell line retains the morphological, phenotypic, and functional properties of normal human microvascular endothelial cells [11, 12], and has been used as an in vitro model to test the cytocompatibility of biomaterials in previous studies [12–14]. For experiments, HMECs were cultured in Dulbecco's minimum essential medium (DMEM, HyClone) supplemented with 10% (v/v) fetal bovine serum (FBS, HyClone) under a 5% CO_2 atmosphere, at 37°C. The cells between passages three and eight after thaw were used for the experiments.

2.8.2 Cell adhesion

HMECs were seeded on chitosan films at 7 × 10^4 cells/cm^2. After incubation for 2 or 4 h, the films were rinsed twice with PBS to remove the unattached cells. Then, the cell adhesion was evaluated by MTT assay. The MTT assay is a measure of the cellular metabolic state, but the activity measured in a culture can be used as an approximation of cell number.

2.8.3 Cell proliferation and morphology

HMECs were seeded on chitosan films at 1 × 10^4 cells/cm^2. Proliferation after 1, 3, and 7 days was determined by MTT assay. After culturing for 2 and 7 days, the cell morphology on the films was observed with an inverted phase contrast microscope (Axiovert 10, Zeiss-Opton, Germany).

2.8.4 Expression of endothelial phenotypic markers

The expression of characteristic endothelial cell markers was investigated by immunofluorescent staining of CD31, vWF, and E-selectin. The immunofluorescent studies were performed on HMECs cultured for 4 days on chitosan films. For investigation of the proinflammatory marker E-selectin, samples were further incubated for 12 h either in the absence or in the presence of TNF-α (1,000 U/ml). The TNF-α was added to induce the E-selectin expression. Briefly, the cells were rinsed with PBS, fixed in 4% (w/v) paraformaldehyde solution for 30 min, permeabilized in 0.1% (v/v) buffered Triton X-100 solution for 20 min, and then blocked in 5% (v/v) normal goat serum for 1 h. The cells were subsequently incubated with mouse anti-human CD31, rabbit anti-human vWF, or mouse anti-human E-selectin for 1 h, and then incubated with the corresponding FITC-conjugated secondary antibodies (YaTai Biotechnology, China) for 1 h. The cell nuclei were counterstained by DAPI (Dojindo, Japan) for 5 min. Finally the samples were observed with a confocal laser-scanning microscope (FV 500, Olympus).

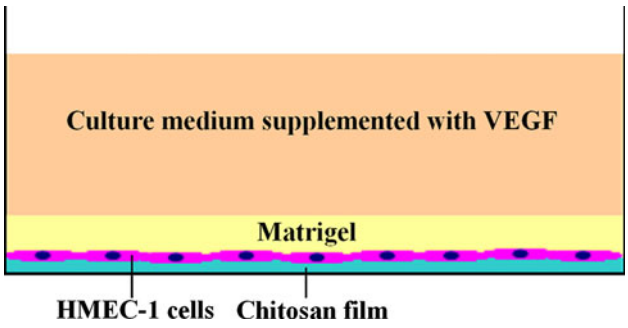

Fig. 1 A schematic diagram for the in vitro angiogenesis assay used in the current study

2.8.5 *Uptake of DiI-Ac-LDL*

HMECs were cultured on chitosan films for 3 days. Then the cells were incubated in culture medium containing DiI-Ac-LDL (10 μg/ml) for 4 h. After the incubation period the cells were washed with PBS and fixed with 4% (w/v) paraformaldehyde solution. Finally, the cells were counterstained by DAPI (Dojindo, Japan) and visualized with a confocal laser-scanning microscope (FV 500, Olympus).

2.8.6 *In vitro angiogenesis assay*

HMECs were cultured on chitosan films for 3 days. Then the cells were covered with Matrigel. Culture medium containing $VEGF_{165}$ (30 ng/ml) was carefully added on top of the gel and incubation was continued (Fig. 1). After 24 h, the cells were fixed in situ with 2% (w/v) paraformaldehyde solution and observed with an inverted phase contrast microscope (Axiovert 10, Zeiss-Opton, Germany). Cell-seeded films cultured without Matrigel under the same conditions were used as controls.

3 Results

3.1 Surface chemistry of chitosan films

ATR-FTIR spectroscopy was used to investigate the surface chemistry of chitosan films. As shown in Fig. 2a, all spectra showed the characteristic peaks of chitosan. The absorption peak at 1,645 cm^{-1} can be assigned to the amide I band, the peak at 1,377 cm^{-1} can be assigned to the amide III band, and the peaks at 1,150 cm^{-1} and 893 cm^{-1} can be assigned to the saccharine structure of chitosan [9, 10, 15]. Both the spectra of Chi-NaOH/H_2O and Chi-NaOH/EtOH films presented a peak at 1,588 cm^{-1}, assigned to the N–H bending vibration of primary amines (amino ($–NH_2$) characteristic peak) [9]. In comparison, the amino characteristic peak of Chi-EtOH film was shifted to the lower wavenumber (observed at 1,582 cm^{-1}), indicating partial protonation of the chitosan [16].

Previous studies indicated that the characteristic peak of protonated amino groups ($–NH_3^+$) on chitosan was at around 1,514 cm^{-1} [17, 18]. Herein, the ratio of absorbance at 1,514 cm^{-1} to that at 1,588 cm^{-1} ($A_{1,514}/A_{1,588}$) was used to evaluate the protonation degree ($–NH_3^+/–NH_2$ ratio) of the chitosan films. As shown in Fig. 2b, the ratio $A_{1,514}/A_{1,588}$ of Chi-EtOH film was obviously higher than those of Chi-NaOH/H_2O and Chi-NaOH/EtOH films, suggesting that the proportion of $–NH_3^+$ groups in the Chi-EtOH film was higher than those in the Chi-NaOH/H_2O and Chi-NaOH/EtOH films.

3.2 Swelling ratios of chitosan films

Figure 3 shows the swelling ratios of chitosan films. Chi-NaOH/EtOH films had the lowest swelling ratio, while Chi-EtOH films had the highest swelling ratio. This result suggests that the structure of the Chi-NaOH/EtOH films was more rigid and compact compared to the Chi-NaOH/H_2O and Chi-EtOH films [10, 19].

3.3 Crystalline conformation of chitosan films

XRD result indicates that neutralization of chitosan films in different solutions resulted in different crystalline conformations (Fig. 4). Chi-NaOH/H_2O film showed a diffraction peak at around 10°, which is the characteristic of "Tendon" (hydrated) polymorph of chitosan [20, 21]. In contrast, Chi-NaOH/EtOH film exhibited a peak at around 15°, which is the characteristic of "Annealed" (anhydrous) polymorph of chitosan [20, 21]. Previous studies indicated that chitosan acetate formed hydrated crystals (called "Type II" crystals) and showed diffraction peaks at 8 and 11° [17, 22]. Herein, Chi-EtOH film exhibited a weak peak at around 8° and a broad peak centered at around 13°. The peak at 8° is attributed to the diffraction of the "Type II" crystals. The peak at 13° can be regarded as a combination of two peaks at 11 and 15°, corresponding to the "Type II" crystals of chitosan acetate and the "Annealed" crystals of chitosan, respectively.

3.4 Surface topography of chitosan films

AFM result shows that chitosan films neutralized in different solutions displayed surface topographies with different nanoscaled features (Fig. 5 and Table 1). Chi-NaOH/H_2O film and Chi-EtOH film had the surfaces consisting of tightly packed particles. Interestingly, for Chi-NaOH/EtOH film, the surface topography was changed

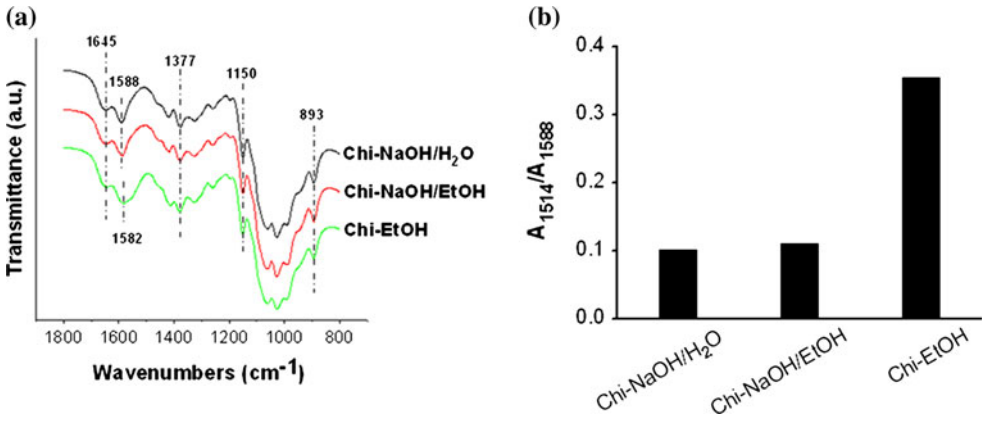

Fig. 2 **a** ATR-FTIR spectra of chitosan films. **b** Ratios of absorbance at 1,514 cm^{-1} to absorbance at 1,588 cm^{-1} of chitosan films

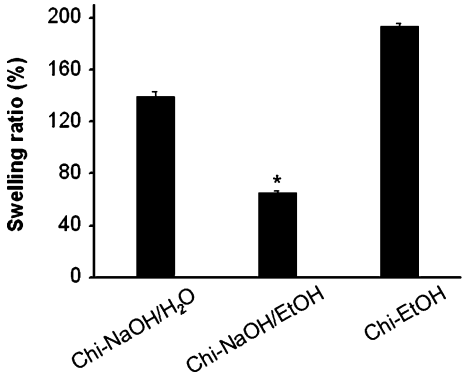

Fig. 3 Swelling ratios of chitosan films. $n = 5$, * $P < 0.001$ relative to the Chi-NaOH/H_2O and Chi-EtOH films

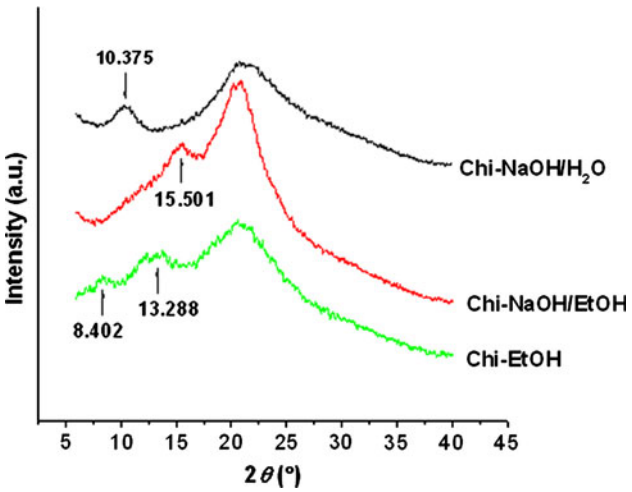

Fig. 4 XRD patterns of chitosan films

to be nanofiber dominant, which was quite different from the Chi-NaOH/H_2O and Chi-EtOH films.

3.5 Mechanical properties of chitosan films

Table 2 indicates that mechanical properties of chitosan films were significantly affected by the neutralizing solutions. The Chi-NaOH/EtOH films showed a higher elastic modulus, a lower elongation-at-break, and a greater tensile strength than the Chi-NaOH/H_2O and Chi-EtOH films, indicating that chitosan films neutralized with NaOH ethanol solution exhibited the highest stiffness.

3.6 Endothelial cell compatibility of chitosan films

3.6.1 Cell adhesion

The adhesion of HMECs increased with increasing incubation time for all samples (Fig. 6). The adhesion of the cells on Chi-NaOH/EtOH films was significantly higher than on Chi-NaOH/H_2O and Chi-EtOH films (Fig. 6).

3.6.2 Cell proliferation

Result shows that the proliferation of HMECs was significantly greater on Chi-NaOH/EtOH films than on Chi-NaOH/H_2O and Chi-EtOH films after 3 and 7 days of culture (Fig. 7), consistent with the result of cell adhesion.

3.6.3 Cell morphology

HMECs exhibited distinctly different morphologies on chitosan films neutralized with different solutions. On Chi-NaOH/H_2O and Chi-EtOH films, the cells retained a spherical shape after a 2-day culture (Fig. 8a, e). Floating cell aggregates were formed by further incubation (Fig. 8b, f). In contrast, cells cultured on Chi-NaOH/EtOH films for 2 days were well spread and showed a fibroblastic morphology (Fig. 8c). After 7 days of culture, these cells grew to confluence and exhibited a typical cobblestone-like morphology on the Chi-NaOH/EtOH films (Fig. 8d).

HMECs cultured on the Chi-NaOH/EtOH films showed significantly improved adhesion and proliferation. Moreover, the cells grown on these chitosan films maintained their endothelial morphology. Therefore, in the following sections, we further analyze the endothelial phenotype and

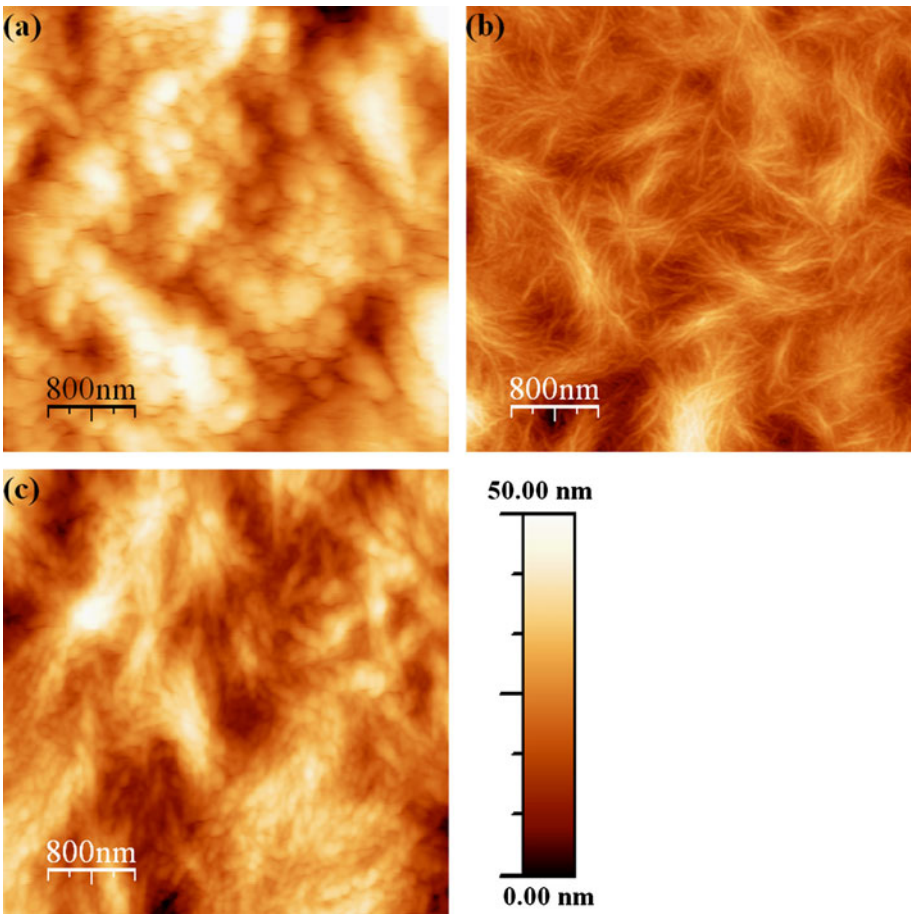

Fig. 5 AFM topographic images of chitosan films. About 4×4 μm^2 size images are shown with z-axis maximum heights of 50 nm. **a** Chi-NaOH/H_2O film, **b** Chi-NaOH/EtOH film, **c** Chi-EtOH film. Notice that the Chi-NaOH/H_2O and Chi-EtOH films displayed particle-dominant surface, while the Chi-NaOH/EtOH film displayed fiber-dominant surface. *Bar* = 800 nm

Table 1 Topography of chitosan films

Sample	Topography	Average length (nm)	Average width (nm)	Average height (nm)
Chi-NaOH/H_2O film	Particle	~265	~180	~32.6
Chi-NaOH/EtOH film	Fiber	~740	~45	~21.2
Chi-EtOH film	Particle	~200	~115	~26.0

Table 2 Tensile mechanical properties of chitosan films ($n = 5$)

Sample	Tensile mechanical property		
	Elastic modulus (MPa)	Elongation-at-break (%)	Tensile strength (MPa)
Chi-NaOH/H_2O film	3.65 ± 0.48	63.74 ± 4.93	1.14 ± 0.10
Chi-NaOH/EtOH film	12.86 ± 1.47*	41.07 ± 6.11*	2.73 ± 0.13*
Chi-EtOH film	1.42 ± 0.19	68.03 ± 5.21	0.62 ± 0.03

* $P < 0.001$ relative to the Chi-NaOH/H_2O and Chi-EtOH films

function of HMECs on the Chi-NaOH/EtOH films. The Chi-NaOH/H_2O and Chi-EtOH films showed poor cell adhesion and proliferation and so will not be further studied here.

3.6.4 Expression of endothelial phenotypic markers

The expression of characteristic endothelial cell markers in HMECs cultured on Chi-NaOH/EtOH films was investigated by immunofluorescent staining of CD31, vWF, and E-selectin. Results show that CD31 was abundantly expressed on the cells (Fig. 9a) [11, 23]. A few of these cells exhibited the typical staining of CD31 located at the intercellular junctions (Fig. 9a, indicated by the arrows) [24]. The cells also revealed the characteristic staining of vWF in the perinuclear region (Fig. 9b) [8]. HMECs cultured in the absence of TNF-α exhibited little or no expression of E-selectin (Fig. 9c), indicating that chitosan induced no inflammatory activation of the endothelial cells, as expected [8]. In contrast, upon incubation with TNF-α, the expression of E-selectin was upregulated (Fig. 9d). Therefore, HMECs cultured on the Chi-NaOH/EtOH films maintained their endothelial phenotype, in terms of expression of these constitutive and inducible markers.

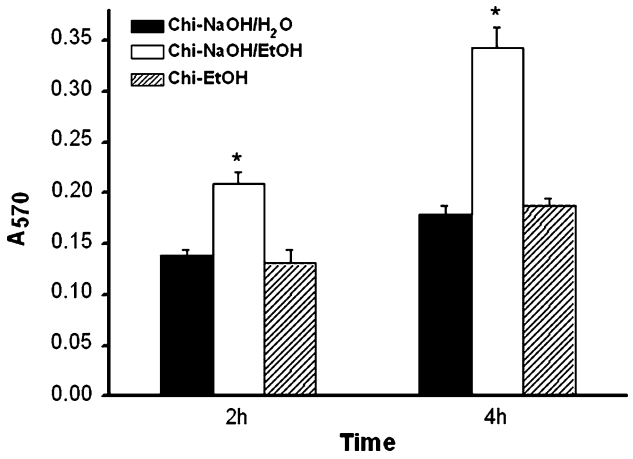

Fig. 6 Adhesion of HMECs on chitosan films. $n = 4$, * $P < 0.001$ relative to the Chi-NaOH/H_2O and Chi-EtOH films

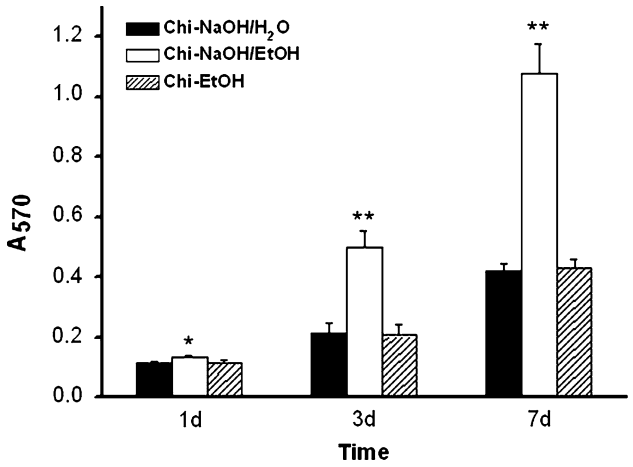

Fig. 7 Proliferation of HMECs on chitosan films. $n = 4$, * $P < 0.05$ relative to the Chi-NaOH/H_2O and Chi-EtOH films, ** $P < 0.001$ relative to the Chi-NaOH/H_2O and Chi-EtOH films

Previous studies have indicated that CD31 is a transmembrane protein constitutively expressed at intercellular junctions on confluent endothelial cells [24, 25]. However, from Fig. 9a, it is noted that not all the HMECs exhibited the concentrated distribution of CD31 at the cell–cell borders. We propose that the CD31 distribution is affected by immortalization of the cells. HMEC-1 cells are immortalized with SV40 T antigen [11]. The T antigen inhibits tumor suppressor proteins p53 and pRb [26, 27], and promotes the activation of mitogen-activated protein kinase (MAPK) pathways [28–32]. The activated MAPKs can phosphorylate cytoskeletal proteins and CD31, leading to disruption of the CD31-cytoskeleton connections and redistribution of the CD31 away from the intercellular junctions [33, 34].

3.6.5 Endothelial function assay

To study the endothelial function of HMECs grown on Chi-NaOH/EtOH films, the capacity of the cells to take up DiI-Ac-LDL and to form capillary-like structures in Matrigel was investigated. Ac-LDL is taken up by endothelial cells through the "scavenger cell pathway" of LDL metabolism, and this metabolism in endothelial cells is shown to be at an accelerated rate compared to other cell types [35]. As shown in Fig. 10a, b HMECs on the Chi-NaOH/EtOH films exhibited a typical punctate fluorescent staining pattern in the perinuclear region, indicating uptake of DiI-Ac-LDL by these cells.

When overlaid with a layer of Matrigel, HMECs migrated from the chitosan film into the gel matrix and formed capillary-like networks within 24 h (Fig. 10c). This indicates the retention of angiogenic potential of the seeded endothelial cells, which is very important for the formation of functional microvasculatures in the cell–chitosan constructs following implantation [8]. As expected, in the absence of Matrigel, capillary-like structures were not observed (Fig. 10d), regardless of VEGF supplementation. Laminin is the major component of Matrigel. When the apical surface of endothelial cells is overlaid with Matrigel, laminin interacts with integrin receptors and promotes migration and angiogenesis [36–38]. Taken together, these results suggest that HMECs grown on Chi-NaOH/EtOH films maintained their endothelial functional properties.

4 Discussion

This study is aimed to prepare chitosan films with good endothelial cell compatibility. For the first time, the effects of different solutions used for neutralization on the physicochemical properties and endothelial cell compatibility of the chitosan films were investigated. Results show that the physicochemical properties and endothelial cell compatibility of the chitosan films were altered by the different neutralizing methods.

NaOH is a strong alkali and it can react with acids completely. Therefore, the amino groups in Chi-NaOH/H_2O and Chi-NaOH/EtOH films were mainly unprotonated. On the other hand, chitosan acetate was hydrolyzed when treated with ethanol solution without NaOH. The generated acetic acid molecules diffused into the ethanol solution and then were removed. However, this hydrolysis reaction is reversible and incomplete; therefore, the amino groups in Chi-EtOH films were partially protonated.

Chitosan is a semicrystalline polysaccharide with inter- and intra-chain hydrogen bonds in polymer matrix. During neutralization in NaOH aqueous solution, incorporation of water molecules into the crystal lattice of Chi-NaOH/H_2O

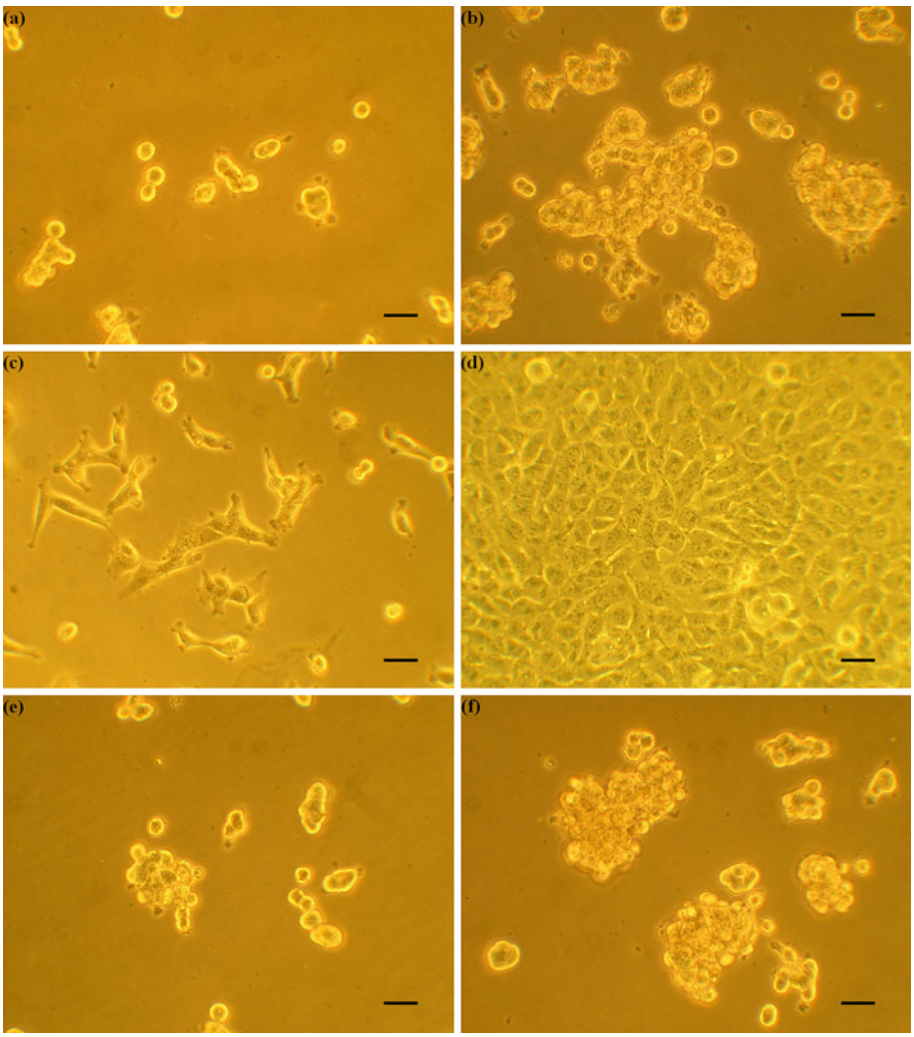

Fig. 8 Micrographs of HMECs cultured on chitosan films for 2 days (**a**, **c**, **e**) and 7 days (**b**, **d**, **f**). **a**, **b** Chi-NaOH/H_2O films, **c**, **d** Chi-NaOH/EtOH films, **e**, **f** Chi-EtOH films. *Bar* = 40 μm

films gave rise to hydrated "Tendon" polymorph, which is the most abundant polymorph of chitosan [21]. In contrast, water molecules were removed when neutralized with NaOH ethanol solution, thereby leading to the formation of anhydrous "Annealed" polymorph in Chi-NaOH/EtOH films. Chi-EtOH films were partially protonated, and contained "Annealed" crystals of chitosan and "Type II" crystals of chitosan acetate. The "Annealed" crystals were formed by simultaneously removing the acetic acid and water molecules from the films by washing with ethanol solution [39]. The presence of the "Type II" crystals was due to the incomplete acid removal. XRD result herein indicates that different neutralizing solutions affected the crystalline conformation of chitosan films; therefore, the chitosan chain arrangements and hydrogen bond patterns are different among these films [39, 40].

One important finding in this study is that different solutions used for neutralization significantly altered the surface nanotopography of chitosan films. Chi-NaOH/EtOH film displayed a nanofiber-dominant surface, while Chi-NaOH/H_2O film and Chi-EtOH film displayed nanoparticle-dominant surfaces. This finding, to our knowledge, has never been reported before in the literature. The change of the surface topography, we assume, can be explained by the above-mentioned differences of the crystalline behavior. Neutralization in different solutions leads to changes in the arrangement and packing of polymer chains, and thereby alters the surface topography of chitosan films [9, 39]. However, further studies are still needed to clarify the exact mechanism.

Another finding of this study is that Chi-NaOH/EtOH films exhibited a higher stiffness than Chi-NaOH/H_2O and Chi-EtOH films. The structure of "Annealed" chitosan polymorph is more compact than that of "Tendon" polymorph because additional inter-chain hydrogen bonds are formed in the "Annealed" crystals upon removal of the water molecules [40–44]. These added inter-chain hydrogen bonds restricted the swelling and enhanced the stiffness of the Chi-NaOH/EtOH films. The Chi-EtOH films also had the "Annealed" crystals. However, the swelling of

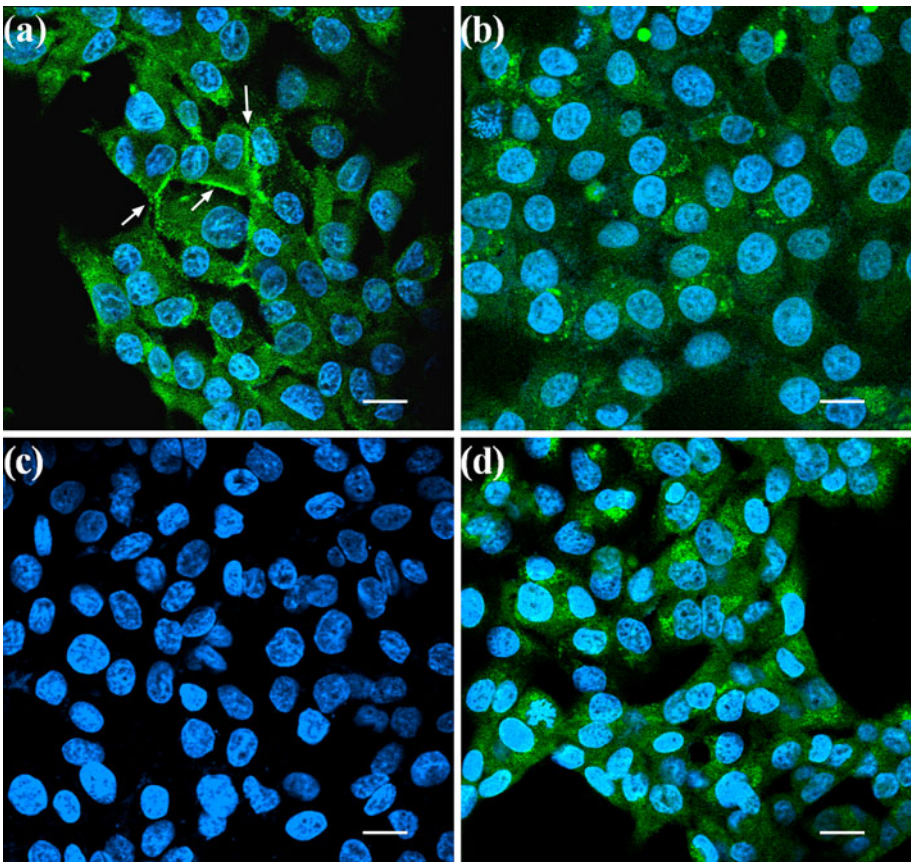

Fig. 9 Immunofluorescent analysis of endothelial phenotypic markers in HMECs grown on Chi-NaOH/EtOH films. Images were collected 4 days after cell seeding. Staining of CD31 (**a**), vWF (**b**), and E-selectin in the absence (**c**) and in the presence (**d**) of TNF-α. *Arrows* indicate localized CD31 staining along the intercellular junctions. *Bar* = 20 μm

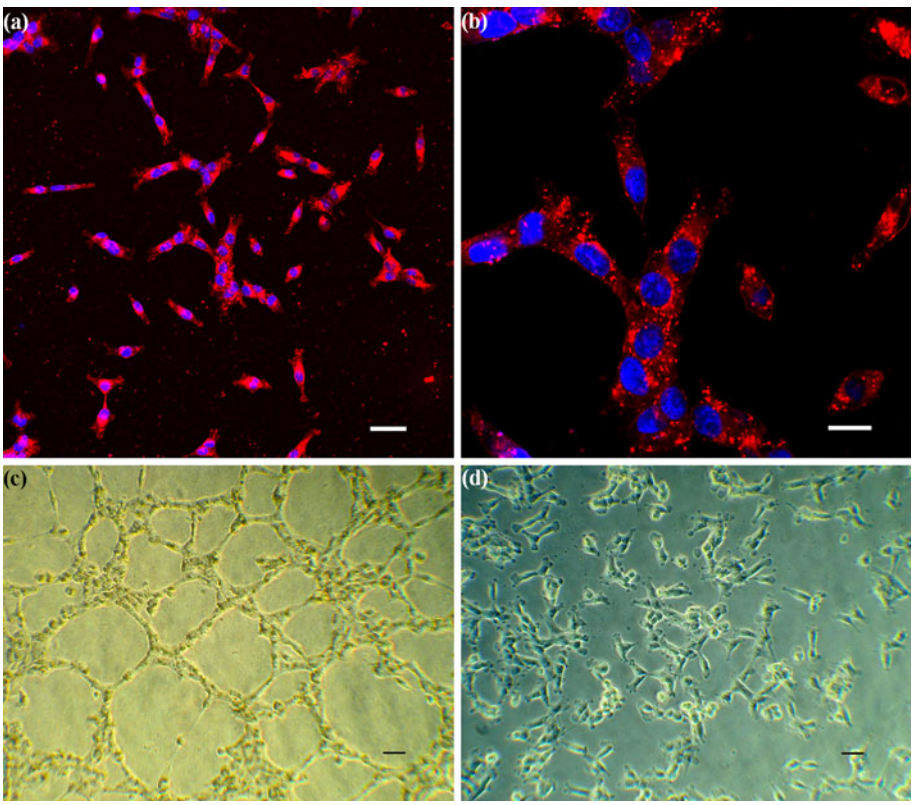

Fig. 10 Functional analysis of HMECs cultured on Chi-NaOH/EtOH films. **a**, **b** Uptake of DiI-Ac-LDL by the cells. **a** *Bar* = 50 μm. **b** *Bar* = 20 μm. **c**, **d** In vitro angiogenesis assay in Matrigel. The cells were incubated with VEGF (30 ng/ml) for 24 h in the presence (**c**) and in the absence (**d**) of Matrigel. **c** *Bar* = 50 μm. **d** *Bar* = 50 μm

the Chi-EtOH films was promoted by ionic repulsion between the protonated amino groups [45], therefore leading to a lower stiffness than the Chi-NaOH/EtOH films.

Cell culture experiments suggest that Chi-NaOH/EtOH films had better endothelial cell compatibility than Chi-NaOH/H_2O and Chi-EtOH films. HMECs cultured on the Chi-NaOH/EtOH films fully spread and exhibited significantly higher levels of adhesion and proliferation. Moreover, the cells grown on the Chi-NaOH/EtOH films maintained their endothelial phenotype and function. It has been reported that cell behavior on biomaterials depends on the physicochemical properties of the substrates [9, 46–49]. Results herein indicate that both surface nanotopography and mechanical properties contributed to determining the endothelial cell compatibility of the chitosan films.

It is reported that fiber-dominant surface mimics the nanoscaled structure of protein fibers in native extracellular matrix (ECM) [9, 50, 51]. In vivo, the ECM structure provides an intricate web of protein nanofibers to support cells and presents an instructive background to guide their behaviors [52–55]. Previous studies indicated that nanofiber matrix could promote the adhesion and proliferation of endothelial cells in vitro [56, 57]. Therefore, the nanofiber topographical cue may produce a driving force for the HMEC adhesion, spreading, and proliferation on the Chi-NaOH/EtOH films. However, the detailed mechanism needs to be further investigated. Substrate stiffness is another important factor in regulating cell behavior. Cells have an integrated mechanotransductory pathway to link the substrate stiffness to the cytoskeletal tension and biochemical signaling pathways. Stiff substrates support cell spreading whereas compliant ones promote rounding, since the substrates with sufficient rigidity can withstand the cell tractional forces generated by cytoskeleton assembly [58, 59]. Therefore, HMECs exhibited enhanced adhesion and spreading on the Chi-NaOH/EtOH films.

5 Conclusions

In this study it is showed for the first time, to our knowledge, that neutralization in different solutions significantly altered the physicochemical properties and endothelial cell compatibility of chitosan films. Chitosan films neutralized with NaOH ethanol solution displayed a nanofiber-dominant surface and exhibited higher stiffness and improved endothelial cell compatibility than the films neutralized with NaOH aqueous solution and the films neutralized with ethanol solution without NaOH. Our findings suggest that the surface nanotopography and mechanical properties contribute to determining the endothelial cell compatibility of the chitosan films. This study provides a further insight into the interactions between chitosan and endothelial cells. The selection of suitable neutralization methods will therefore be highly important for the use of chitosan in tissue engineering.

Acknowledgments This study was supported by grants from The National Natural Science Foundation of China (30700848, 30772443), The National Basic Research Program of China ("973 Program", 2005CB623905) and The National Natural Science Foundation of Beijing (7082090).

References

1. Suh JK, Matthew HW. Application of chitosan-based polysaccharide biomaterials in cartilage tissue engineering: a review. Biomaterials. 2000;21:2589–98.
2. Martino AD, Sittinger M, Risbud MV. Chitosan: a versatile biopolymer for orthopaedic tissue-engineering. Biomaterials. 2005;26:5983–90.
3. Ao Q, Wang A, Cao W, Zhang L, Kong L, He Q, Gong Y, Zhang X. Manufacture of multimicrotubule chitosan nerve conduits with novel molds and characterization in vitro. J Biomed Mater Res A. 2006;77A:11–8.
4. Moon JJ, West JL. Vascularization of engineered tissues: approaches to promote angiogenesis in biomaterials. Curr Top Med Chem. 2008;8:300–10.
5. Unger RE, Peters K, Wolf M, Motta A, Migliaresi C, Kirkpatrick CJ. Endothelialization of a non-woven silk fibroin net for use in tissue engineering: growth and gene regulation of human endothelial cells. Biomaterials. 2004;25:5137–46.
6. Chupa JM, Foster AM, Sumner SR, Madihally SV, Matthew HW. Vascular cell responses to polysaccharide materials: in vitro and in vivo evaluations. Biomaterials. 2000;21:2315–22.
7. Chung TW, Lu YF, Wang SS, Lin YS, Chu SH. Growth of human endothelial cells on photochemically grafted Gly-Arg-Gly-Asp (GRGD) chitosans. Biomaterials. 2002;23:4803–9.
8. Amaral IF, Unger RE, Fuchs S, Mendonca AM, Sousa SR, Barbosa MA, Pego AP, Kirkpatrick CJ. Fibronectin-mediated endothelialisation of chitosan porous matrices. Biomaterials. 2009;30:5465–75.
9. Zheng Z, Zhang L, Kong L, Wang A, Gong Y, Zhang X. The behavior of MC3T3–E1 cells on chitosan/poly-L-lysine composite films: effect of nanotopography, surface chemistry, and wettability. J Biomed Mater Res A. 2009;89A:453–65.
10. Cheng M, Deng J, Yang F, Gong Y, Zhao N, Zhang X. Study on physical properties and nerve cell affinity of composite films from chitosan and gelatin solutions. Biomaterials. 2003;24:2871–80.
11. Ades EW, Candal FJ, Swerlick RA, George VG, Summers S, Bosse DC, Lawley TJ. HMEC-1: establishment of an immortalized human microvascular endothelial cell line. J Invest Dermatol. 1992;99:683–90.
12. Shin M, Matsuda K, Ishii O, Terai H, Kaazempur-Mofrad M, Borenstein J, Detmar M, Vacanti JP. Endothelialized networks with a vascular geometry in microfabricated poly (dimethyl siloxane). Biomed Microdevices. 2004;6:269–78.
13. Hakimi O, Gheysens T, Vollrath F, Grahn MF, Knight DP, Vadgama P. Modulation of cell growth on exposure to silkworm and spider silk fibers. J Biomed Mater Res A. 2010;92A:1366–72.
14. Ogwu AA, Okpalugo TIT, Ali N, Maguire PD, McLaughlin JAD. Endothelial cell growth on silicon modified hydrogenated amorphous carbon thin films. J Biomed Mater Res B. 2008;85B:105–13.

15. Xu J, McCarthy SP, Gross RA. Chitosan film acylation and effects on biodegradability. Macromolecules. 1996;29:3436–40.
16. Katti KS, Katti DR, Dash R. Synthesis and characterization of a novel chitosan/montmorillonite/hydroxyapatite nanocomposite for bone tissue engineering. Biomed Mater. 2008;3:034122.
17. Demarger-Andre S, Domard A. Chitosan carboxylic acid salts in solution and in the solid state. Carbohyd Polym. 1994;23:211–9.
18. Osman Z, Arof AK. FTIR studies of chitosan acetate based polymer electrolytes. Electrochim Acta. 2003;48:993–9.
19. Cao W, Jing D, Li J, Gong Y, Zhao N, Zhang X. Effects of the degree of deacetylation on the physicochemical properties and Schwann cell affinity of chitosan films. J Biomater Appl. 2005; 20:157–77.
20. Ogawa K, Yui T, Miya M. Dependence on the preparation procedure of the polymorphism and crystalline of chitosan membranes. Biosci Biotechnol Biochem. 1992;56:858–62.
21. Ogawa K. Effect of heating an aqueous suspension of chitosan on the crystallinity and polymorphs. Agric Biol Chem. 1991;55: 2375–9.
22. Yamamoto A, Kawada J, Yui T, Ogawa K. Conformation behavior of chitosan in the acetate salt: an X-ray study. Biosci Biotechnol Biochem. 1997;61:1230–2.
23. van Beijnum JR, van der Linden E, Griffioen AW. Angiogenic profiling and comparison of immortalized endothelial cells for functional genomics. Exp Cell Res. 2008;314:264–72.
24. Peters K, Unger RE, Stumpf S, Schafer J, Tsaryk R, Hoffmann B, Eisenbarth E, Breme J, Ziegler G, Kirkpatrick CJ. Cell type-specific aspects in biocompatibility testing: the intercellular contact in vitro as an indicator for endothelial cell compatibility. J Mater Sci Mater Med. 2008;19:1637–44.
25. Vestweber D. Molecular mechanisms that control endothelial cell contacts. J Pathol. 2000;190:281–91.
26. Jha KK, Banga S, Palejwala V, Ozer HL. SV40-mediated immortalization. Exp Cell Res. 1998;245:1–7.
27. Cheng J, DeCaprio JA, Fluck MM, Schaffhausen BS. Cellular transformation by simian virus 40 and murine polyoma virus T antigens. Semin Cancer Biol. 2009;19:218–28.
28. Marchetti A, Cecchinelli B, D'Angelo M, D'Orazi G, Crescenzi M, Sacchi A, Soddu S. p53 can inhibit cell proliferation through caspase-mediated cleavage of ERK2/MAPK. Cell Death Differ. 2004;11:596–607.
29. Gottifredi V, Pelicci G, Munarriz E, Maione R, Pelicci PG, Amati P. Polyomavirus large T antigen induces alterations in cytoplasmic signalling pathways involving Shc activation. J Virol. 1999;73:1427–37.
30. Fei ZL, D'Ambrosio C, Li S, Surmacz E, Baserga R. Association of insulin receptor substrate 1 with simian virus 40 large T antigen. Mol Cell Biol. 1995;15:4232–9.
31. Weng LP, Smith WM, Brown JL, Eng C. PTEN inhibits insulin-stimulated MEK/MAPK activation and cell growth by blocking IRS-1 phosphorylation and IRS-1/Grb-2/Sos complex formation in a breast cancer model. Hum Mol Genet. 2001;10:605–16.
32. Wu GS. The functional interactions between the p53 and MAPK signaling pathways. Cancer Biol Ther. 2004;3:156–61.
33. Ferrero E, Bondanza A, Leone BE, Manici S, Poggi A, Zocchi MR. $CD14^{+}CD34^{+}$ peripheral blood mononuclear cells migrate across endothelium and give rise to immunostimulatory dendritic cells. J Immunol. 1998;160:2675–83.
34. Ferrero E, Villa A, Ferrero ME, Toninelli E, Bender JR, Pardi R, Zocchi MR. Tumor necrosis factor α-induced vascular leakage involves PECAM1 phosphorylation. Cancer Res. 1996;56: 3211–5.
35. Janic B, Guo AM, Iskander ASM, Varma NRS, Scicli AG, Arbab AS. Human cord blood-derived AC133 + progenitor cells preserve endothelial progenitor characteristics after long term in vitro expansion. PLoS ONE. 2010;5:e9173.
36. Kubota Y, Kleinman HK, Martin GR, Lawley TJ. Role of laminin and basement membrane in the morphological differentiation of human endothelial ceils into capillary-like structures. J Cell Biol. 1988;107:1589–98.
37. Chalupowicz DG, Chowdhury ZA, Bach TL, Barsigian C, Martinez J. Fibrin II induces endothelial cell capillary tube formation. J Cell Biol. 1995;130:207–15.
38. Kumar VBS, Viji RI, Kiran MS, Sudhakaran PR. Modulation of expression of LDH isoenzymes in endothelial cells by laminin: implications for angiogenesis. J Cell Biochem. 2008;103: 1808–25.
39. Ogawa K, Yui T, Okuyama K. Three D structures of chitosan. Int J Biol Macromol. 2004;34:1–8.
40. Kawada J, Yui T, Okuyama K, Ogawa K. Crystalline behavior of chitosan organic acid salts. Biosci Biotechnol Biochem. 2001;65: 2542–7.
41. Notin L, Viton C, David L, Alcouffe P, Rochas C, Domard A. Morphology and mechanical properties of chitosan fibers obtained by gel-spinning: influence of the dry-jet-stretching step and ageing. Acta Biomater. 2006;2:387–402.
42. Yamaguchi I, Itoh S, Suzuki M, Sakane M, Osaka A, Tanaka J. The chitosan prepared from crab tendon I: the characterization and the mechanical properties. Biomaterials. 2003;24:2031–6.
43. Osorio-Madrazo A, David L, Trombotto S, Lucas JM, Peniche-Covas C, Domard A. Kinetics study of the solid-state acid hydrolysis of chitosan: evolution of the crystallinity and macromolecular structure. Biomacromolecules. 2010;11: 1376–86.
44. Ogawa K, Hirano S, Miyanishi T, Yui T, Watanabe T. A new polymorph of chitosan. Macromolecules. 1984;17:973–5.
45. Wang QZ, Chen XG, Li ZX, Wang S, Liu CS, Meng XH, Liu CG, Lv YH, Yu LJ. Preparation and blood coagulation evaluation of chitosan microspheres. J Mater Sci Mater Med. 2008;19: 1371–7.
46. Singhvi R, Stephanopoulos G, Wang DI. Effects of substratum morphology on cell physiology. Biotechnol Bioeng. 1994;43: 764–71.
47. Lydon MJ, Minett TW, Tighe BJ. Cellular interactions with synthetic polymer surfaces in culture. Biomaterials. 1985;6: 396–402.
48. Flemming RG, Murphy CJ, Abrams GA, Goodman SL, Nealey PF. Effects of synthetic micro- and nano-structured surfaces on cell behavior. Biomaterials. 1999;20:573–88.
49. Ingber DE, Folkman J. Mechanochemical switching between growth and differentiation during fibroblast growth factor-stimulated angiogenesis in vitro: role of extracellular matrix. J Cell Biol. 1989;109:317–30.
50. Chu XH, Shi XL, Feng ZQ, Gu ZZ, Ding YT. Chitosan nanofiber scaffold enhances hepatocytes adhesion and function. Biotechnol Lett. 2009;31:347–52.
51. Ma Z, Kotaki M, Inai R, Ramakrishna S. Potential of nanofiber matrix as tissue-engineering scaffolds. Tissue Eng. 2005;11: 101–9.
52. Scott JE. Extracellular matrix, supramolecular organization and shape. J Anat. 1995;187:259–69.
53. Zagris N. Extracellular matrix in development of the early embryo. Micron. 2001;32:427–38.
54. Abrams GA, Goodman SL, Nealey PF, Franco M, Murphy CJ. Nanoscale topography of the basement membrane underlying the corneal epithelium of the rhesus macaque. Cell Tissue Res. 2000; 299:39–46.
55. Toh YC, Ng S, Khong YM, Zhang X, Zhu Y, Lin PC, Te CM, Sun W, Yu H. Cellular responses to a nanofibrous environment. Nano Today. 2006;1:34–43.
56. Feng ZQ, Lu HJ, Leach MK, Huang NP, Wang YC, Liu CJ, Gu ZZ. The influence of type-I collagen-coated PLLA aligned

nanofibers on growth of blood outgrowth endothelial cells. Biomed Mater. 2010;5:065011.
57. Francois S, Chakfe N, Durand B, Laroche G. A poly (L-lactic acid) nanofibre mesh scaffold for endothelial cells on vascular prostheses. Acta Biomater. 2009;5:2418–28.
58. Yeung T, Georges PC, Flanagan LA, Marg B, Ortiz M, Funaki M, Zahir N, Ming W, Weaver V, Janmey PA. Effects of substrate stiffness on cell morphology, cytoskeletal structure, and adhesion. Cell Motil Cytoskel. 2005;60:24–34.
59. Thompson MT, Berg MC, Tobias IS, Rubner MF, van Vliet KJ. Tuning compliance of nanoscale polyelectrolyte multilayers to modulate cell adhesion. Biomaterials. 2005;26:6836–45.